Linearized quantum transport equations: ac conductance of a quantum wire with an electron-phonon interaction

Petr Král
Institute of Physics, Academy of Sciences, Na Slovance 2, 180 40 Praha 8, Czech Republic
(Received 6 September 1995)

A linear response formalism is developed for evaluation of transport coefficients in quantum many-particle systems. The method is based on a systematic linearization of nonequilibrium Kadanoff-Baym transport equations in an *integral* form in ac electric fields. Simple and consistent approximations can be performed in the resulting set of transport equations, which replace vertex equations in the Kubo formalism. The method is illustrated by the example of an ac and dc conductivity and conductance for a quasi-one-dimensional electron system with an electron–phonon interaction for three-dimensional acoustical phonons. After approximations standard in metals, the solved transport equations coincide with the Holstein equation.

I. INTRODUCTION

Transport phenomena in quantum many-particle systems, in particular with a restricted geometry, cannot be fully understood without quantum transport theory, which would be simple and reliable, but at the same time powerful enough to avoid inappropriate approximations. The nonequilibrium Green's functions formalism (NGF) of Kadanoff and Baym[1] and Keldysh[2] can faithfully describe quantum systems in nonequilibrium.[3] Unfortunately, the complex structure of the theory involving double time structure was slowing down an application of NGF. Therefore, much effort has been devoted to reduce NGF in strongly nonequilibrium systems to a single time transport theory.[4]

Very successful are applications of the NGF to a derivation of linear response formalisms of a general validity, where usually the double time structure can be avoided. In NGF the Dyson equation in complex times and in the presence of external fields is analytically continued to real times.[5] This gives a set of transport equations for nonequilibrium correlation functions in either a *differential*[1] or an *integral* form.[6] Linearization of these transport equations in terms of the external fields produces new equations, from which the linear response coefficients can be found.

In equilibrium systems these theories can be compared with the complementary approach of the Kubo formula,[7] which expresses the linear response in terms of a special type of a two-particle Green's function. One way of its actual determination is to linearize the one-particle Matsubara Green's functions[8] with respect to the external fields. This gives a Bethe-Salpeter equation[9] for the two-particle Green's function of complex times. Its solution can be, after an analytic continuation to real times, identified with the Kubo formula with minimal vertex corrections.[9]

Several works followed the way of linearized NGF with the goal of developing a simple consistent scheme of incorporating approximations for carrier scattering. Linearized Kadanoff-Baym transport equations in a *differential* form for dc electric fields have been used by Prange and Kadanoff[10] for an electron-phonon interaction. Hänsch and Mahan[11] have elaborated and applied this approach. Their results reproduced correctly the Holstein equation[12] for the electron-phonon scattering in the Migdal approximation. Chen and Su[13] have tried to augment this method to achieve a proper bookkeeping of the many terms appearing as a result of the approximate linearization of the *differential* form. This extension is unavoidable for more complicated types of scattering. Another generalization of the method[11] is to the case of the ac electric fields, by Wu and Mahan.[14] The last method does not explicitly coincide with the work[11] in the dc limit $\omega \to 0$, but the Holstein equation[12] (the Boltzmann limit) has been acquired too. A gauge invariant form of these *differential* equations has been recently presented by Levanda and Fleurov,[15] where the ac equations coincide in the limit $\omega \to 0$ with the dc equations.

In this work we linearize quantum transport equations in the *integral* form.[16] This way is probably more flexible than the *differential* methods,[11,15] because some intermediate steps can be avoided and the resulting system of equations appears simpler. The *integral* approach is also inherent to the Kubo formula, but in our method one and two-particle points of view are more clearly interconnected. This opens a possibility to easily perform consistent approximations. When testing equilibrium systems, the new method seems to agree with the Kubo formula for minimal vertex corrections.[9] The approach can be applied in stationary nonequilibrium conditions, and its possible extension to transient nonequilibrium situations is ensured by its NGF origin.

We apply the new method to evaluate ac and dc conductivity and conductance for a quasi-one-dimensional (1D) electron system, embedded in a three-dimensional (3D) semiconductor and interacting with bulk acoustical phonons.[17] After standard approximations for metals, the method gives the Holstein equation[12] for this model. Its numerical solutions show that below $T \approx 1$ K scattering of electrons in a backward direction freezes out and the homogeneous dc conductivity, given solely by scattering in a forward direction, goes like T^{-3}. Similar phenomena appear also in the homogeneous or inhomogeneous ac conductivity. From the conductivity we evaluate an ac/dc conductance, defined by an absorbed power in a locally excited part of the wire.[18] The one-channel dc conductance acquires the stan-

 © 1996 The American Physical Society

dard value $2e^2/h$ as $T\rightarrow 0$ K. Above $T\approx 1$ K this conductance sharply falls down, due to the presence of the backward scattering. Here the ac conductance grows as a function of a frequency until the backward scattering becomes disturbed.

The paper is organized as follows. In Sec. II we develop the new linear response method from the quantum transport equations in the integral form. We linearize these equations and explain how transport coefficients can be evaluated from the linearized transport equations in a frequency-momentum representation. In Sec. IV we apply the new method to evaluation of an ac/dc conductivity and conductance for a quasi-1D electron system with an electron-phonon interaction. In this section some numerical results are presented, which might be of importance for mesoscopics. In Appendix B we show how conservation laws result for the linearized functions in the new method. The equivalence of the new linearized transport equations with the Holstein equation is also presented there for our model. Finally relaxation times are evaluated from the solutions of the linearized transport equations.

II. LINEARIZED KADANOFF-BAYM EQUATIONS IN THE INTEGRAL FORM

Consider an interacting electron system excited by an electromagnetic field. This system can be described by the Hamiltonian

$$H=H_s+H_{\rm ext},$$

$$H_{\rm ext}=e\int d^3\mathbf{r}\ \varphi(\mathbf{r},t)\rho(\mathbf{r})-\frac{e}{c}\int d^3\mathbf{r}\ \mathbf{A}(\mathbf{r},t)\cdot\mathbf{j}(\mathbf{r})+\frac{e^2}{2mc^2}\int d^3\mathbf{r}\ \mathbf{A}^2(\mathbf{r},t)\rho(\mathbf{r}), \tag{1}$$

where H_s is the Hamiltonian for the free system and $H_{\rm ext}$ represents coupling to the fields, described by the scalar $\varphi(\mathbf{r},t)$ or the vector potential $\mathbf{A}(\mathbf{r},t)$. In the following we will assume that the fields are weak, so that without loss of generality the potentials can be used in the forms

$$\varphi(\mathbf{r},t)=\varphi_0 e^{-i(\omega t-\mathbf{k}\cdot\mathbf{r})+\delta t},$$

$$\mathbf{A}(\mathbf{r},t)=\mathbf{E}_0 c\frac{e^{-i(\omega t-\mathbf{k}\cdot\mathbf{r})+\delta t}}{i\omega}\quad(\delta\rightarrow 0). \tag{2}$$

The density $\rho(\mathbf{r})$ and the current density operators $\mathbf{j}(\mathbf{r})$ are[9]

$$\rho(\mathbf{r})=\psi^+(\mathbf{r})\psi(\mathbf{r}),$$

$$\mathbf{j}(\mathbf{r})=\frac{\hbar}{2im}[\psi^+(\mathbf{r})\nabla\psi(\mathbf{r})-(\nabla\psi^+(\mathbf{r}))\psi(\mathbf{r})]. \tag{3}$$

For our purposes it is appropriate to describe the system by Green's functions, time ordered along a curve in the complex plane[5] (generalization of the Matsubara GF). The electron Green's function follows a Dyson equation in the integral or differential form. Its inverted solution looks like

$$G^{-1}(1,2)=G_0^{-1}(1,2)-U(1,2)-\Sigma(1,2), \tag{4}$$

$$U(1,2)=\delta(t_1-t_2)\left(e\phi(1)-\frac{e\hbar}{2cim}\mathbf{A}(1)\cdot(\nabla_{r_1}-\nabla_{r_2})+\frac{e^2}{2mc^2}\mathbf{A}^2(1)\right),$$

where the numbers $j=1,2$ represent a pair of coordinates $(\mathbf{r}_j,t_j)$. The fields (2) are characterized by the operator function $U(1,2)$, which is implicitly present also in the self-energy $\Sigma(1,2)$ (some GF relationships are summarized in Appendix A).

A. Formulation of the equations

Linear response coefficients can be precisely calculated from the Bethe-Salpeter equation[9] (Kubo formula) or the *differential* form of the Kadanoff-Baym equations.[1] Our starting point in the linearization scheme is the *integral* version of the Kadanoff-Baym transport equations (A10).

The NGF origin of these equations allows their application to strongly nonequilibrium systems. Here for simplicity we consider that the studied system is in stationary nonequilibrium conditions, maintained by the external fields and by a contact with reservoir. Then initial condition contained in the function $G_0^<$ dies out and the nonequilibrium transport equations (A10) become simplified as follows:

$$G^<(1,2)=G^r(1,\bar{3})\Sigma^<(\bar{3},\bar{4})G^a(\bar{4},2). \tag{5}$$

The equation for $G^>$ results by the exchange of $\Sigma^<$ by $\Sigma^>$ in (5), so that only the equation for $G^<$ ($\delta G^</\delta U$) will be written as a representative of the pair of equations for $G^<$, $G^>$ ($\delta G^</\delta U, \delta G^>/\delta U$). The nonequilibrium propagators $G^{r,a}(1,2)$ can be found from $G^{<,>}(1,2)$ by (A3).

In this work we consider that the weak probe fields (2) test an *equilibrium* system. Term by term variation of (5) over these fields φ or $\mathbf{A}$ gives a new set of equations

$$\begin{aligned}\frac{\delta G^<(1,1')}{\delta U(2)}&=\hat{\mathbf{p}}_U[G^r(1,2)G^<(2',1')+G^<(1,2)G^a(2',1')]_{2'=2}\\&+G^r(1,\bar{3})\frac{\delta\Sigma^r(\bar{3},\bar{4})}{\delta U(2)}G^<(\bar{4},1')\\&+G^<(1,\bar{3})\frac{\delta\Sigma^a(\bar{3},\bar{4})}{\delta U(2)}G^a(\bar{4},1')\\&+G^r(1,\bar{3})\frac{\delta\Sigma^<(\bar{3},\bar{4})}{\delta U(2)}G^a(\bar{4},1').\end{aligned} \tag{6}$$

In (6) the functional derivative of $G^{r(a)}$ was substituted by the identity[9]

$$\frac{\delta G^r(1,1')}{\delta U(2)}=\hat{\mathbf{p}}_U[G^r(1,2)G^r(2',1')]_{2'=2}+G^r(1,\bar{3})\frac{\delta\Sigma^r(\bar{3},\bar{4})}{\delta U(2)}G^r(\bar{4},1'), \tag{7}$$

where the formulas

$$\frac{\delta G^r(1,3)}{\delta U(2,4)} \equiv -G^r(1,\bar{5})\frac{\delta (G^r)^{-1}(\bar{5},\bar{6})}{\delta U(2,4)} G^r(\bar{6},3) \tag{8}$$

and (4) were used. The operator is $\hat{\mathbf{p}}_U = 1$, $(\hbar/2im)\times(\nabla_2 - \nabla_{2'})$ for $U = e\varphi$, $-(e/c)\mathbf{A}$, and the nonlinear term in $\mathbf{A}^2$ is neglected due to weakness of the probe fields. The single particle functions $G^{<,>,r,a}$ in (6), (7) are taken in equilibrium.

The linearized propagators $\delta G^{r,a}/\delta U$ could also be expressed from the linearized correlation functions $\delta G^{<,>}/\delta U$ in an equivalency analogical to that between the propagators $G^{r,a}$ and the correlation functions $G^{<,>}$ (see Appendix A)

$$\frac{\delta G^r(1,1')}{\delta U(2)} = -\frac{i}{\hbar}\Theta(1-1')\left(\frac{\delta G^>(1,1')}{\delta U(2)} + \frac{\delta G^<(1,1')}{\delta U(2)}\right). \tag{9}$$

If the expressions for the linearized correlation functions from (6) and its counterpart $\delta G^>/\delta U$ are inserted into (9), then, after some algebra with theta functions, the right side of (7) results. Therefore (7) and (9) are equivalent to each other and are consistent with the transport equations (6).

From the identity (9) an important relation between the linearized functions results. If we take into account that $G^r(1^+,1) = 1$, then it follows that

$$\frac{\delta G^r(1^+,1)}{\delta U(2)} = -\frac{i}{\hbar}\Theta(1^+-1)\frac{\delta A(1,1)}{\delta U(2)} = 0, \qquad \frac{\delta G^>(1,1)}{\delta U(2)} = -\frac{\delta G^<(1,1)}{\delta U(2)}. \tag{10}$$

In other words as $1' \to 1$ the two linearized correlation functions degenerate into one. The linear response coefficients can be found from the function $\delta G^<(1,1)/\delta U(2)$. To obtain this function of one argument $(1-2)$ (for a stationary and homogeneous system), the more general function $\delta G^<(1,3)/\delta U(2)$ with two arguments $(1-3),(1-2)$ must be found. Therefore the equivalency (10) usually does not reduce the number of solved equations, but in some systems it gives a hint to a possible simplification.

The coupled system of transport equations (6) and its counterpart for $\delta G^>/\delta U$ will be closed, if all functions are expressed by $\delta G^{<,>}/\delta U$. This can be achieved in two steps. First the functions $\delta\Sigma^{r,a}/\delta U$ should be represented by $\delta\Sigma^{<,>}/\delta U$ in a relation analogous to (A6) and (A7), holding between $\Sigma^{r,a}$ and $\Sigma^{<,>}$. Second the functions $\delta\Sigma^{<,>}/\delta U$ must be expressed by $\delta G^{<,>}/\delta U$ in the same way as relate $\Sigma^{<,>}$ and $G^{<,>}$ for a given many-body approximation.

Let us see these relationships in more details. Generally the electron self-energy is a sum of the *singular* (Hartree-Fock or mean field) part $\Sigma_{\rm HF}$ and the *regular* or collisional part[1] Σ_c. Both parts contribute to the self-energy propagators, but only the *regular* part has nonzero contribution to the correlation function of the self-energy

$$\Sigma^r(1,3) = \Sigma^r_{\rm HF}(1,3) + \Sigma^r_c(1,3), \quad \Sigma^<(1,3) = \Sigma^<_c(1,3). \tag{11}$$

The linearized self-energy function fulfills the same relationships

$$\frac{\delta\Sigma^r(1,3)}{\delta U(2)} = \frac{\delta\Sigma^r_{\rm HF}(1,3)}{\delta U(2)} + \frac{\delta\Sigma^r_c(1,3)}{\delta U(2)}, \qquad \frac{\delta\Sigma^<(1,3)}{\delta U(2)} = \frac{\delta\Sigma^<_c(1,3)}{\delta U(2)}. \tag{12}$$

The Hartree-Fock self-energy, which is a mean field approximation local in time of the electron-electron interactions, has the retarded part equal to

$$\Sigma^r_{\rm HF}(1,3) = \delta(t_1-t_3)\,\delta(\mathbf{r}_1-\mathbf{r}_3)\int d^3\bar{\mathbf{r}}\, v(\mathbf{r}_1-\bar{\mathbf{r}}) \times G^<(\bar{\mathbf{r}},t_1;\bar{\mathbf{r}},t_1) + \delta(t_1-t_3)v(\mathbf{r}_1-\mathbf{r}_3) \times G^<(\mathbf{r}_1,t_1;\mathbf{r}_3,t_1). \tag{13}$$

This propagator self-energy can be linearized as follows:

$$\frac{\delta\Sigma^r_{\rm HF}(1,3)}{\delta U(2)} = \delta(t_1-t_3)\,\delta(\mathbf{r}_1-\mathbf{r}_3)\int d^3\bar{\mathbf{r}}\, v(\mathbf{r}_1-\bar{\mathbf{r}}) \times \frac{\delta G^<(\bar{\mathbf{r}},t_1;\bar{\mathbf{r}},t_1)}{\delta U(2)} + \delta(t_1-t_3)v(\mathbf{r}_1-\mathbf{r}_3) \times \frac{\delta G^<(\mathbf{r}_1,t_1;\mathbf{r}_3,t_1)}{\delta U(2)}. \tag{14}$$

The collisional contributions fulfill the same relationships as the related self-energy parts, namely (A6) and (A7)

$$\frac{\delta\Sigma^r_c(1,3)}{\delta U(2)} = -\frac{i}{h}\Theta(t_1-t_3)\left(\frac{\delta\Sigma^>_c(1,3)}{\delta U(2)} + \frac{\delta\Sigma^<_c(1,3)}{\delta U(2)}\right). \tag{15}$$

Generation of linear response functions by a functional derivative is known to lead in a safe way to many-body *conserving* approximations[1] (conservation laws are fulfilled[9]). To ensure this mandatory consistency of the transport equations in the presence of approximations, the same approximative steps must be performed in $\Sigma^{<,>}$ and $\delta\Sigma^{<,>}/\delta U$. This holds not only for the approximations, which result by selecting an appropriate class of Feynman diagrams in the self-energy,[19] but also for auxiliary physically motivated approximations. This makes it possible to keep under control a self-consistent structure of the one- and two-particle levels of the solution. Some of these approximations are presented in the next section.

B. Frequency representation

Weak probe fields can be resolved into Fourier components (2), which can be considered to act on the studied system independently. A linear response to composite weak fields can be calculated from a linear superposition of responses to Fourier components of these fields. Since the weakly excited system remains space and time translationally invariant, it is enough to know any linearized function

$\delta F(1,3)/\delta U(2)$, from the transport equations (6), for the differences of arguments $(1-3)$, $(1-2)$. Our results can be more simply compared with the work of Holstein,[12] if we define the Fourier transform in a little unsymmetric way

$$\frac{\delta F(1,3)}{\delta U(2)} = \int_{-\infty}^{\infty} \frac{d\omega_1}{2\pi} \int_{-\infty}^{\infty} \frac{d\omega_2}{2\pi} \int_{-\infty}^{\infty} \frac{d\mathbf{k}_1}{2\pi} \int_{-\infty}^{\infty} \frac{d\mathbf{k}_2}{2\pi} \frac{\delta F}{\delta U}(\omega_1,\mathbf{k}_1;\omega_2,\mathbf{k}_2) \times \exp\left[i\omega_1(t_1-t_3) + i\omega_2(t_1-t_2) - i\mathbf{k}_1\cdot(\mathbf{r}_1-\mathbf{r}_3) - i\mathbf{k}_2\cdot\left(\frac{\mathbf{r}_1+\mathbf{r}_3}{2}-\mathbf{r}_2\right)\right]. \tag{16}$$

Internal arguments of the functions $(\omega_1,\mathbf{k}_1)$ are analogical as in $G(\mathbf{k},\omega)$. External arguments $(\omega_2,\mathbf{k}_2)$ are identical with those in the fields (2).

Application of the transform (16) to Eqs. (6) gives

$$\begin{aligned}\frac{\delta G^<}{\delta U}(\mathbf{k}_1,\omega_1;\mathbf{k}_2,\omega_2) = {} & G^r\left(\mathbf{k}_1+\frac{\mathbf{k}_2}{2},\omega_1+\omega_2\right)\left(\mathbf{p}_U+\frac{\delta\Sigma^r}{\delta U}(\mathbf{k}_1,\omega_1;\mathbf{k}_2,\omega_2)\right)G^<\left(\mathbf{k}_1-\frac{\mathbf{k}_2}{2},\omega_1\right) \\ & + G^<\left(\mathbf{k}_1+\frac{\mathbf{k}_2}{2},\omega_1+\omega_2\right)\left(\mathbf{p}_U+\frac{\delta\Sigma^a}{\delta U}(\mathbf{k}_1,\omega_1;\mathbf{k}_2,\omega_2)\right)G^a\left(\mathbf{k}_1-\frac{\mathbf{k}_2}{2},\omega_1\right) \\ & + G^r\left(\mathbf{k}_1+\frac{\mathbf{k}_2}{2},\omega_1+\omega_2\right)\frac{\delta\Sigma^<}{\delta U}(\mathbf{k}_1,\omega_1;\mathbf{k}_2,\omega_2)G^a\left(\mathbf{k}_1-\frac{\mathbf{k}_2}{2},\omega_1\right),\end{aligned} \tag{17}$$

where the functional derivative of G^r was substituted by

$$\begin{aligned}\frac{\delta G^r}{\delta U}(\mathbf{k}_1,\omega_1;\mathbf{k}_2,\omega_2) = {} & G^r\left(\mathbf{k}_1+\frac{\mathbf{k}_2}{2},\omega_1+\omega_2\right) \\ & \times\left(\mathbf{p}_U+\frac{\delta\Sigma^r}{\delta U}(\mathbf{k}_1,\omega_1;\mathbf{k}_2,\omega_2)\right) \\ & \times G^r\left(\mathbf{k}_1-\frac{\mathbf{k}_2}{2},\omega_1\right)\end{aligned} \tag{18}$$

and the momentum is $\mathbf{p}_U=1,\ \hbar\mathbf{k}_1/m$ for $U=e\varphi,-(e/c)\mathbf{A}$.

Later we will also use the relationship (15) in a frequency representation

$$\begin{aligned}\frac{\delta\Sigma_c^r}{\delta U}(\omega_1;\omega_2) = {} & \frac{1}{2\pi}\int\frac{d\bar{\omega}}{\omega_1-\bar{\omega}+i\delta} \\ & \times\left(\frac{\delta\Sigma_c^>}{\delta U}(\bar{\omega};\omega_2)+\frac{\delta\Sigma_c^<}{\delta U}(\bar{\omega};\omega_2)\right).\end{aligned} \tag{19}$$

Here we have written only the frequency variables.

C. Transport coefficients

Transport coefficients can be easily calculated from the solution of the transport equations (17). For example the total current density induced by weak probe fields results by averaging of the velocity of electrons over the perturbed state of the system[20]

$$\begin{aligned}\mathbf{J}(\mathbf{r},t) &= e\left\langle \mathbf{j}(\mathbf{r},t) - \frac{e}{mc}\mathbf{A}(\mathbf{r},t)\rho(\mathbf{r})\right\rangle \\ &= \mathbf{J}_{\rm corr}(\mathbf{r},t)+\mathbf{J}_{\rm diam}(\mathbf{r},t) \\ &= \int d^3\bar{\mathbf{r}}\,d\bar{t}\;\sigma(\mathbf{r}-\bar{\mathbf{r}},t-\bar{t})\cdot\mathbf{E}(\bar{\mathbf{r}},\bar{t}),\end{aligned} \tag{20}$$

where the definitions (3) have been applied. Averaging of the current density operator $\mathbf{j}$ gives the correlation current $\mathbf{J}_{\rm corr}$ and averaging of the product of the vector potential $\mathbf{A}$ with the density operator ρ gives the diamagnetic current $\mathbf{J}_{\rm diam}$. The correlation current can be expressed in a frequency-momentum representation as follows:

$$\begin{aligned}\mathbf{J}_{\rm corr}(\mathbf{k},\omega) &= e\int\frac{d^3\hbar\bar{\mathbf{k}}}{(2\pi)^3}\frac{\hbar\bar{\mathbf{k}}}{m}\int\frac{d\bar{\omega}}{2\pi}G^<(\bar{\mathbf{k}},\bar{\omega}) \\ &= e\int\frac{d^3\hbar\bar{\mathbf{k}}}{(2\pi)^3}\frac{\hbar\bar{\mathbf{k}}}{m}\int\frac{d\bar{\omega}}{2\pi}\left\{ G_0^<(\bar{\mathbf{k}},\bar{\omega}) \right. \\ &\quad + \frac{\delta G^<}{\delta\left(-\frac{e}{c}\mathbf{A}\right)}(\bar{\mathbf{k}},\bar{\omega};\mathbf{k},\omega) \\ &\quad \left.\times\left(-\frac{e}{c}\mathbf{A}(\mathbf{k},\omega)\right)+\cdots\right\}.\end{aligned} \tag{21}$$

Combination of the formulas (20) and (21) together with the relation between frequency components of the electric field and vector potential $\mathbf{E}=(i\omega/c)\mathbf{A}$ gives the components of the tensor for ac conductivity

$$\sigma_{\alpha,\beta}(\mathbf{k},\omega)=\frac{i}{\omega}\left(\frac{n_0e^2}{m}\delta_{\alpha,\beta}+\Pi^{\mathrm{r}}_{\alpha,\beta}(\mathbf{k},\omega)\right),$$

$$\Pi^{r}_{\alpha,\beta}(\mathbf{k},\omega)=\frac{2ie}{\omega}\int\frac{d^3\hbar\bar{\mathbf{k}}}{(2\pi)^3}\frac{\hbar\bar{k}_\alpha}{m}\times\int\frac{d\bar{\omega}}{2\pi}\frac{\delta G^{<}}{\delta\left(-\frac{e}{c}A_\beta\right)}(\bar{\mathbf{k}},\bar{\omega};\mathbf{k},\omega). \quad (22)$$

Here n_0 is the concentration of carriers and the multiplication by 2 results from the summation over spin components. In many situations only the diagonal elements of the conductivity tensor are nonzero.

Another physical property which is often required is the polarizability of a quantum many-body system.[20] It can be calculated from the transport equations (17) as the linear response to the scalar potential ϕ. The polarizability differs from the correlation part in (22) by deletion of the momentum prefactor and the substitution of $\delta G^{<}/\delta\mathbf{A}$ by $\delta G^{<}/\delta\phi$. In the Appendix B we show how conservation laws are fulfilled by the linear response functions $\delta G^{<}/\delta\mathbf{A}$ and $\delta G^{<}/\delta\phi$.

The question remains whether the resulting linear response coefficients are equivalent to those found by the Kubo formula. To answer this question in full generality would be quite hard, because different analytical structures in both methods lead to different diagrammatic expansions. Therefore more work is necessary in this direction in the future.

III. ELECTRON-PHONON INTERACTION IN QUASI-1D

In order to see how the linearized transport equations (17) can be applied, we find an ac/dc conductivity and conductance for a quasi-1D electron system. The model has been introduced and studied in Ref. 17, where one-particle properties and the nonvertex conductivity and conductance have been investigated. Later a multiband extension of the model was also presented.[21] In our work we evaluate vertex corrections to the conductivity from Ref. 17 by the new linear response method.

The system is a single-quantum-well wire formed in a bulk semiconductor. The wire is extended in the z direction and confined by a rotationally symmetric parabolic potential in the x,y directions. The longitudinal motion along the wire can be described by plane waves with wave vectors from a 1D band with a parabolic dispersion relation. The transverse motion of electrons is quantized into harmonic oscillator states. The electrons in this quasi-1D system are coupled to longitudinal 3D acoustic phonons.[20]

Here we discuss for simplicity only transport in the lowest state of the well. This one-band model can be described by the modified Frőhlich Hamiltonian[12,16]

$$H=\sum_k\frac{\hbar^2k^2}{2m}a_k^+a_k+\sum_q\hbar s|q|b_q^+b_q+\sum_{k,q_l}a_k^+a_{k-q_l}\sum_{q_t}F(q_t)M(q)(b_q+b_{-q}^+), \quad (23)$$

$$F(q_t)=\exp\left(-\frac{\sigma_0^2(q_x^2+q_y^2)}{4}\right),$$

$$M(q)=-V_0|q|\left(\frac{1}{2\rho_{\mathrm{cryst}}s|q|}\right)^{1/2},$$

where the ground state of the well is characterized by the wave function

$$\psi(x,y)=\frac{1}{\sigma_0\sqrt{\pi}}\exp\left(-\frac{x^2+y^2}{2\sigma_0^2}\right). \quad (24)$$

In (23) s is the velocity of sound, σ_0 is the diameter of the wire, ρ_{cryst} is the density of matter, and V_0 is the strength of the electron-phonon interaction.[20] The operator a_k^+ creates an electron with a 1D wave vector k in the transversal state (24) and the operator b_q^+ creates an acoustical phonon with a 3D wave vector $q=(q_x,q_y,q_{z=l})$, $q_t^2=q_x^2+q_y^2$. In this work the electron-phonon interaction in (23) as well as the probing longitudinal field from (2) are not screened.

A. One-particle properties

Electrons and phonons in this system can be described by 1D-electron and 3D-phonon Green's functions (see the Appendix A). The influence of the quasi-1D electrons on the 3D phonons is probably small, so that the renormalization of phonons is neglected.[22,12] In experiments the Fermi level is usually high enough, which means that the electrons on this level are much faster than sound. Therefore the Migdal approximation of the electron self-energy should be valid (possible breakdown is mentioned later)

$$\Sigma(k;t,t')=-i\sum_{q_l,q_t}(F(q_t)M(q))^2G(k-q_l;t,t')D(q;t,t'). \quad (25)$$

Its correlation function $\Sigma^{<}$ can be written as

$$\Sigma^{<}(k,\omega)=\frac{1}{(2\pi)^4}\int d\bar{\omega}\,d\bar{q}_l\,d^2\bar{q}_t(F(\bar{q}_t)M(\bar{q}))^2\times G^{<}(k-\bar{q}_l,\omega-\bar{\omega})D^{<}(\bar{q},\bar{\omega})$$
$$=\int_{-\infty}^{\infty}\frac{d\bar{\omega}}{2\pi}\int_{-\infty}^{\infty}\frac{d\bar{q}_l}{2\pi}A(k-\bar{q}_l,\omega-\bar{\omega})\times\mathscr{A}(\bar{q}_l,\bar{\omega})n_F(\hbar\omega-\hbar\bar{\omega})n_B(\hbar\bar{\omega}), \quad (26)$$

where we have used the expressions (A5) and (A9). The function $\mathscr{A}(q_l,\omega)$ can be found from the δ-like spectral function for 3D free phonons

$$A_D(q,\omega)=2\pi[\delta(\hbar\omega-\hbar\omega_q)-\delta(\hbar\omega+\hbar\omega_q)]$$
$$=\frac{2\pi\omega}{\hbar s^2\sqrt{(\omega/s)^2-q_l^2}}\delta\left(|q_t|-\sqrt{\left(\frac{\omega}{s}\right)^2-q_l^2}\right)\times\Theta\left[\left(\frac{\omega}{s}\right)^2-q_l^2\right]. \quad (27)$$

In the second expression of (27) the amplitude of the transversal momentum $|q_t|$ has been chosen as a new variable.

TABLE I. Parameters of the model.

effective electron mass	$m = 0.0165\ m_e$
density (bulk GaAs)	$\rho_{\text{cryst}} = 4560$ kg/m^3
velocity of a sound	$s = 5220$ m/s
interaction constant	$V_0 = 7$ eV
diameter of the wire	$\sigma_0 = 7$ nm
Fermi energy	$E_F = 20$ meV

Substituting the function $A_D(k,\omega)$ from (27) into (26) and performing the integration over q_l, the function $\mathscr{A}(q_l,\omega)$ results as follows:

$$\mathscr{A}(q_l,\omega) = C_i|\omega|\omega \exp\left\{-\frac{\sigma_0^2}{2}\left[\left(\frac{\omega}{s}\right)^2 - q_l^2\right]\right\} \times \Theta\left[\left(\frac{\omega}{s}\right)^2 - q_l^2\right]. \tag{28}$$

The correlations functions $\Sigma^<$, $\Sigma^>$ differ only by statistical factors and the retarded self-energy Σ^r can be calculated from them as in the Appendix A.

We have numerically tested the non-self-consistent form of the Migdal self-energy, called the first-order Tamm-Dankoff (TD1) approximation, which results from (26) by application of free Green's functions. These tests, with parameters in Table I, show that the magnitude of $\mathrm{Im}\,\Sigma^r$ is about 10^{-2} meV, but the structure in $\mathrm{Im}\,\Sigma^r$ has the width of the order of meV. Therefore the self-consistent electron spectral function should be sharply localized around E_F, so the renormalization constant is very close to one, $Z_0 \approx 0.99$, and the Migdal self-energy could be apparently substituted by the TD1 self-energy. The tests also show that the TD1 self-energy (26) depends very weakly on the wave vector k, because the momentum dependence for the effective phonon spectral function $\mathscr{A}$ is much weaker than that for the spectral function for electrons A due to the small s/v_F ratio. Therefore the TD1 self-energy can be further approximated by keeping constant the integration variable $\bar{q}_l$ in $\mathscr{A}$ during the $\bar{q}_l$ integration. Since the electron dispersion law in 1D has two branches (around $k \approx \pm k_F$), the $\bar{q}_l$ integration can be divided into two parts. They naturally separate the scattering in the forward and backward directions, for which the constants in $\mathscr{A}$ can be chosen as $\bar{q}_l = 0$ and $\bar{q}_l = 2k_F$. By this approximation the k variable can be integrated out from the electron spectral function $A(k-\bar{q}_l, \omega-\bar{\omega})$ in (26), so the correlation function $\Sigma^<$ becomes k independent

$$\Sigma^<(\omega) = \int_{-\infty}^{\infty} \frac{d\bar{\omega}}{2\pi} \frac{\Theta(\hbar\omega - \hbar\bar{\omega} + \mu)}{\sqrt{\frac{2\hbar^2}{m}(\hbar\omega - \hbar\bar{\omega} + \mu)}} \times [F_f(\bar{\omega}) + F_b(\bar{\omega})] n_F(\hbar\omega - \hbar\bar{\omega}) n_B(\hbar\bar{\omega}), \tag{29}$$

$$F_f(\bar{\omega}) \equiv C_i|\bar{\omega}|\bar{\omega} \exp\left[-\frac{\sigma_0^2}{2}\left(\frac{\bar{\omega}}{s}\right)^2\right],$$

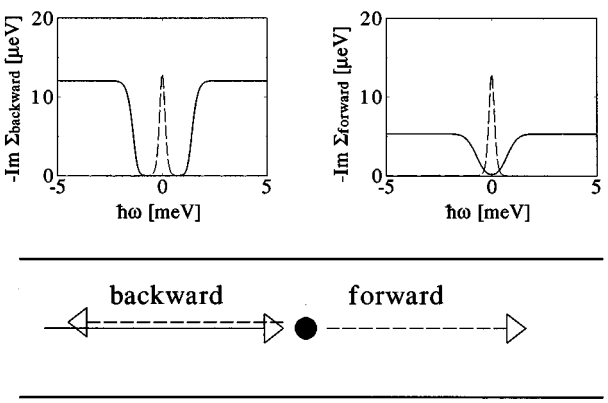


FIG. 1. Schematic draft of the electron scattering on acoustical phonons in the quasi-1D system. In the insets we can see contributions to the imaginary part of the self-energy $\mathrm{Im}\,\Sigma^r$, as a function of energy, from scattering in the forward and backward directions. A linearized electron dispersion law has been used and the temperature is $T = 1$ K. As $T \to 0$ K the Luttinger theorem is fulfilled, so that $\mathrm{Im}\,\Sigma^r(E_F) \to 0$. The dashed line represents a derivative of a Fermi-Dirac distribution at the same temperature.

$$F_b(\bar{\omega}) \equiv C_i|\bar{\omega}|\bar{\omega} \exp\left\{-\frac{\sigma_0^2}{2}\left[\left(\frac{\bar{\omega}}{s}\right)^2 - (2k_F)^2\right]\right\} \times \Theta\left[\left(\frac{\bar{\omega}}{s}\right)^2 - (2k_F)^2\right].$$

Here the functions $F_f(\omega)$ and $F_b(\omega)$ are effective scattering factors in the forward and backward directions. The above substitutions *preserve* inelastic character of the scattering in this model. They are analogous to the momentum-indepedent approximation of a self-energy,[10] called also the first quasi-classical approximation.

In Fig. 1 we demonstrate scattering of electrons in the forward and backward directions. Contributions from these two scattering channels to the self-energy in (29) are presented in the upper insets for parameters in Table I. In the forward scattering phonons of very low momenta $\bar{q}_l \approx 0$ (and only these) can be excited. Therefore it is $\mathrm{Im}\,\Sigma^r_{\text{forward}}(\omega) \neq 0$ even very closely to the Fermi energy (see the right inset). In a strictly 1D system one-phonon scattering of electrons in the forward direction is completely forbidden by conservation conditions, so that the forward scattering can reappear only in higher orders of a perturbation theory.[23] In the studied quasi-1D model, momentum conservation rules are broken [see (28)], so that a weakly inelastic one-phonon forward scattering is present. In the elastic approximation the forward scattering falls out completely.[24]

In the backward part $\mathrm{Im}\,\Sigma^r_{\text{backward}}$ a gap is present around the Fermi level, where $\mathrm{Im}\,\Sigma^r_{\text{backward}} \approx 0$ at low temperatures. The gap has a half-width $2sk_F$ (see the left inset), given by scattering on phonons with momenta $\bar{q}_l \approx 2k_F$. The distribution function $dn_F(\hbar\omega)/d\omega$, from a conductivity formula, is localized around E_F and has the half-width $\hbar\omega \approx k_{\text{Bol}}T$. Therefore at low temperatures this distribution practically does not overlap with the backward self-energy contribution

$\mathrm{Im}\,\Sigma^r_{\mathrm{backward}}$, so that the backward scattering freezes out below the temperature $T_f = 2sk_F/k_{\mathrm{Bol}}$ (≈ 14 K here). At lower temperatures, tails of the distribution $dn_F(\hbar\omega)/d\omega$ have only exponentially small overlap with the backward part of $\mathrm{Im}\,\Sigma^r$ and the forward scattering must dominate (here at $T \approx 1$ K).

B. Two-particle properties

We can find the linearized transport equations (17) for the present model, probed by the weak longitudinal electric field $\mathbf{A}(\mathbf{r},t) = \mathbf{E}_0 c[e^{-i(\omega t - \mathbf{k}\cdot\mathbf{r}) + \delta t}/i\omega]$ ($\mathbf{k}$ is parallel to $\mathbf{A}$ and to the wire). This vector potential $\mathbf{A}(\mathbf{r},t)$ can represent one Fourier component of the longitudinal electric field, which appears below a slit irradiated by a laser beam.[17]

To keep the approach self-consistent, the Migdal approximation of the self-energy (26) must be applied also in linearized self-energy functions from Eqs. (17). In this many-body approximation the function $\delta\Sigma^</\delta\mathbf{A}$ looks like [we use a simplified notation $-(e/c)\mathbf{A}\to\mathbf{A}$]

$$\frac{\delta\Sigma^<}{\delta\mathbf{A}}(k_1,\omega_1;k_2,\omega_2) = \int \frac{d\bar{\omega}}{2\pi}\int \frac{d\bar{q}_l}{2\pi}\frac{\delta G^<}{\delta\mathbf{A}}(k_1-\bar{q}_l,\omega_1-\bar{\omega};k_2,\omega_2) \times \mathscr{A}(\bar{q}_l,\bar{\omega}) n_B(\hbar\bar{\omega}). \tag{30}$$

We have to perform in $\delta\Sigma^</\delta\mathbf{A}$ all other approximations applied before to $\Sigma^<$. In (29) the integration variable $\bar{q}_l$ in the function $\mathscr{A}$ is substituted by two rigid values $\bar{q}_l = 0$ and $\bar{q}_l = 2k_F$, for the forward and backward scattering, and the $\bar{q}_l$ integration is performed around these values. If the same substitutions are performed in (30), then the k_1-independent function $\delta\Sigma^</\delta\mathbf{A}$ results

$$\frac{\delta\Sigma^<}{\delta\mathbf{A}_\pm}(\omega_1;k_2,\omega_2) = \int \frac{d\bar{\omega}}{2\pi} n_B(\hbar\bar{\omega}) \times\left(F_f(\bar{\omega})\frac{\delta G^<}{\delta\mathbf{A}_\pm}(\omega_1-\bar{\omega};k_2,\omega_2) + F_b(\bar{\omega})\frac{\delta G^<}{\delta\mathbf{A}_\mp}(\omega_1-\bar{\omega};k_2,\omega_2)\right), \tag{31}$$

where the k_1-independent (but the sign of k_1) linearized functions are defined by

$$\frac{\delta G^<}{\delta\mathbf{A}_\pm}(\omega_1;k_2,\omega_2) = \int_\pm \frac{d\bar{k}_1}{2\pi}\frac{\delta G^<}{\delta\mathbf{A}}(\bar{k}_1,\omega_1;k_2,\omega_2). \tag{32}$$

Here the signs $\pm$ mean integration in the neighborhood of the values $\bar{k}_1 = \pm k_F$, which correspond to the two branches of the electron dispersion law in 1D. Note that these signs are reversed in the second term of (31). The k_1-independent linearized propagators for a self-energy $\delta\Sigma^{r,a}/\delta\mathbf{A}$ relate to $\delta\Sigma^{<,>}/\delta\mathbf{A}$ by (15). If Eqs. (17) for the present model are integrated as in (32), then a new closed system of equations for $(\delta G^{<,>}/\delta\mathbf{A}_\pm)(\omega_1;k_2,\omega_2)$ can be derived.

Let us see this directly. If the above derived k_1-independent linearized self-energy functions in (31) are substituted in (17), then on the right side of this equation the variable k_1 appears only in the pairs of Green's functions. Therefore, when the $\bar{k}_1$ integration from (32) is applied to (17), these pairs of Green's functions can be integrated separately from other terms. These integrals of bilinear combinations of propagators and correlation functions are performed below.

To simplify integrations of these functions, the dispersion law for electrons E_k can be linearized in the neighborhood of the Fermi wave vectors as follows:[20]

$$E_k = \frac{\hbar^2[(k\mp k_f)\pm k_f]^2}{2m} \approx \mu \pm C_0(k\mp k_f), \qquad C_0 = \frac{\hbar^2 k_F}{m} = \hbar v_F. \tag{33}$$

The same approximation has been done in the self-energy (29) from Fig. 1. In fact at the Fermi level, where transport is important, this approximation changes the self-energy very little. The approximate propagator results

$$G^r_\pm(k,\omega) = \frac{1}{\hbar\omega - E_k + \mu - \Sigma^r(\omega)} \approx \mp\frac{1}{C_0}\frac{1}{k\mp\alpha}, \qquad \alpha \equiv k_F + \frac{\hbar\omega - \mu + \mu - \Sigma^r(\omega)}{C_0}, \tag{34}$$

and the functions $G^a_\pm(k,\omega)$ and $G^{<,>}_\pm(k,\omega)$ can be expressed from (34).

The integrals from bilinear combinations of the approximate Green's functions can be easily evaluated

$$\begin{aligned} I_1^\pm(\omega_1;k_2,\omega_2) &\equiv \int_\pm \frac{d\bar{k}_1}{2\pi} G^r_\pm(\bar{k}_1+k_2/2,\omega_1+\omega_2)G^a_\pm(\bar{k}_1-k_2/2,\omega_1) \\ &\doteq \frac{1}{C_0^2}\int_{-\infty}^{\infty}\frac{d\bar{k}_1}{2\pi}\frac{1}{\bar{k}_1+k_2/2\mp\alpha(\omega_1+\omega_2)} \times\frac{1}{\bar{k}_1-k_2/2\mp\alpha^*(\omega_1)} \\ &= \mp\frac{i}{C_0}\frac{1}{(C_0k_2\mp\hbar\omega_2)\mp(\Sigma^r(\omega_1+\omega_2)-\Sigma^a(\omega_1))}, \end{aligned}$$

$$\begin{aligned} I_2^\pm(\omega_1;k_2,\omega_2) &\equiv \int_\pm \frac{d\bar{k}_1}{2\pi} G^<_\pm(\bar{k}_1+k_2/2,\omega_1+\omega_2) \times G^a_\pm(\bar{k}_1-k_2/2,\omega_1) \\ &\doteq i n_F(\hbar\omega_1+\hbar\omega_2) I_1^\pm(\omega_1;k_2,\omega_2), \end{aligned}$$

$$\begin{aligned} I_3^\pm(\omega_1;k_2,\omega_2) &\equiv \int_\pm \frac{d\bar{k}_1}{2\pi} G^r_\pm(\bar{k}_1+k_2/2,\omega_1+\omega_2) \times G^<_\pm(\bar{k}_1-k_2/2,\omega_1) \\ &\doteq -i n_F(\hbar\omega_1) I_1^\pm(\omega_1;k_2,\omega_2). \end{aligned} \tag{35}$$

After the selection of one of the values $\bar{k}_1 \approx \pm k_F$, the integrations in (35) can be directly performed. Extension of the integration interval from one of the branches of the electron dispersion law to the the whole real axis of $\bar{k}_1$ makes probably only small errors.

These integrals can be used to define the new set of coupled equations [analogously the equation for $(\delta G^{>}/\delta \mathbf{A}_{\pm})(\omega_1;k_2,\omega_2)$ results]

$$\frac{\delta G^{<}}{\delta \mathbf{A}_{\pm}}(\omega_1;k_2,\omega_2) = \left(\pm\frac{\hbar k_F}{m} + \frac{\delta \Sigma^{r}}{\delta \mathbf{A}_{\pm}}(\omega_1;k_2,\omega_2) \right) I_3^{\pm}(\omega_1;k_2,\omega_2) + \left(\pm\frac{\hbar k_F}{m} + \frac{\delta \Sigma^{a}}{\delta \mathbf{A}_{\pm}}(\omega_1;k_2,\omega_2) \right) I_2^{\pm}(\omega_1;k_2,\omega_2) + I_1^{\pm}(\omega_1;k_2,\omega_2)\frac{\delta \Sigma^{<}}{\delta \mathbf{A}_{\pm}}(\omega_1;k_2,\omega_2). \tag{36}$$

In (36) the momentum prefactor is approximated by the Fermi momentum and taken out of the integrals.

Application of the solution of (36) in the formula (22), little modified for the present case, gives the ac conductivity

$$\sigma(k,\omega) = \frac{2i\hbar e^2}{\omega} v_F \int_{-\infty}^{\infty} \frac{d\bar{\omega}}{2\pi} \left(\frac{\delta G^{<}}{\delta \mathbf{A}_{+}}(\bar{\omega};k,\omega) - \frac{\delta G^{<}}{\delta \mathbf{A}_{-}}(\bar{\omega};k,\omega) \right). \tag{37}$$

Note that the corellation part of the conductivity (37) does not cancel the diamagnetic term in (22), due to the approximations of the integrals (35) (see also Ref. 20). Fortunately the diamagnetic term does not influence the experimentally accessible real part of the conductivity.

C. Reduction to one transport equation

In (10) we have shown that

$$\frac{\delta G^{>}(1,3)}{\delta U(2)} \to -\frac{\delta G^{<}(1,3)}{\delta U(2)} \quad \text{as} \quad 3 \to 1.$$

After a Fourier transform to the momentum-frequency representation $(k_1,\omega_1;k_2,\omega_2)$ in (16), this equivalency is not fulfilled by separate frequency components, but only by their integral over the frequency ω_1. It is interesting that the ω_1 integration could be effectively substituted in this role by the k_1 integration in (32). If we apply in (36) and its counterpart for $(\delta G^{>}/\delta \mathbf{A}_{\pm})(\omega_1;k_2,\omega_2)$ the identity (19) and the relations (35) between $I^{\pm}_{1,2,3}$, then after some little algebra the mentioned equivalency results

$$\frac{\delta G^{>}}{\delta \mathbf{A}_{\pm}}(\omega_1;k_2,\omega_2) = -\frac{\delta G^{<}}{\delta \mathbf{A}_{\pm}}(\omega_1;k_2,\omega_2),$$

$$\frac{\delta G^{r,a}}{\delta \mathbf{A}_{\pm}}(\omega_1;k_2,\omega_2) = 0. \tag{38}$$

Fulfillment of (38) is a consequence of the quasi-local character of our interaction, which gives a very weak momentum dependent electron self-energy. This dependence can be neglected and the necessary ω_1-energy integration, leading to (10), can be shifted to the k_1-momentum integration, due to the unambiguous pole relationship in (34).

Relations (38) reduce the system of linearized transport equations to one equation, which is derived here for the electron-phonon interaction. By the relationships (38) and the equivalency (19) the linearized propagators for a self-energy can be expressed from (31) and its counterpart for $\delta \Sigma^{>}/\delta \mathbf{A}_{\pm}$ as follows:

$$\frac{\delta \Sigma^{r,a}}{\delta \mathbf{A}_{\pm}}(\omega_1;k_2,\omega_2) = -\frac{1}{2\pi}\int \frac{d\bar{\omega}}{\omega_1 - \bar{\omega} \pm i\delta} \int \frac{d\bar{\omega}_1}{2\pi} \left(F_f(\bar{\omega}_1)\frac{\delta G^{<}}{\delta \mathbf{A}_{\pm}}(\bar{\omega}-\bar{\omega}_1;k_2,\omega_2) + F_b(\bar{\omega}_1)\frac{\delta G^{<}}{\delta \mathbf{A}_{\mp}}(\bar{\omega}-\bar{\omega}_1;k_2,\omega_2) \right). \tag{39}$$

We can substitute the expressions (39) into the transport equation (36), multiply both its sides by the inverted function $I_1^{\pm}(\omega_1;k_2,\omega_2)$, and reorder terms. Then this single transport equation has the form

$$\begin{aligned} & iC_0[\pm C_0 k_2 - \hbar\omega_2 + \Sigma^{r}(\omega_1+\omega_2) - \Sigma^{a}(\omega_1)]\frac{\delta G^{<}}{\delta \mathbf{A}_{\pm}}(\omega_1;k_2,\omega_2) \\ &= \pm\frac{i\hbar k_F}{m}[n_F(\hbar\omega_1+\hbar\omega_2) - n_F(\hbar\omega_1)] + \int \frac{d\bar{\omega}_1}{2\pi} \left(\frac{n_F(\hbar\omega_1+\hbar\omega_2) + n_F(\hbar\omega_1)}{2} + n_B(\hbar\bar{\omega}_1) \right) \\ &\quad \times \left(F_f(\bar{\omega}_1)\frac{\delta G^{<}}{\delta \mathbf{A}_{\pm}}(\omega_1-\bar{\omega}_1;k_2,\omega_2) + F_b(\bar{\omega}_1)\frac{\delta G^{<}}{\delta \mathbf{A}_{\mp}}(\omega_1-\bar{\omega}_1;k_2,\omega_2) \right) + i[n_F(\hbar\omega_1) - n_F(\hbar\omega_1+\hbar\omega_2)] \\ &\quad \times \int \frac{d\bar{\omega}}{2\pi}\frac{1}{\omega_1-\bar{\omega}} \int \frac{d\bar{\omega}_1}{2\pi} \left(F_f(\bar{\omega}_1)\frac{\delta G^{<}}{\delta \mathbf{A}_{\pm}}(\bar{\omega}-\bar{\omega}_1;k_2,\omega_2) + F_b(\bar{\omega}_1)\frac{\delta G^{<}}{\delta \mathbf{A}_{\mp}}(\bar{\omega}-\bar{\omega}_1;k_2,\omega_2) \right). \end{aligned} \tag{40}$$

Equation (40) is similar to the Holstein equation,[12] derived for the electron–phonon interaction with acoustical phonons, but in (40) no limitation to the strength of the interaction has been applied. The validity of these equations is probably the same as equations in Ref. 10.

For not very strong interactions a pole approximation for a self-energy sometimes called the second quasiclassical approximation, can be applied. For weak interactions the quasiparticle spectrum can be substituted by a free particle spectrum. In (40) this can be performed as follows: $\hbar\omega_1 \approx e_{k_1}-\mu$, $(\mu \equiv E_F)$, $\hbar\bar{\omega}_1 \approx e_{k_1}-e_{k_1-q_l}$, and $\hbar d\bar{\omega}_1 \approx \hbar v_k\, dq_l = C_0\, dq_l$. This substitution diminishes the frequency variable ω_1 and reinstalls the integrated out k_1 variable. It would seem that the frequency variable ω_1 could be integrated out from $\Sigma^r(k_1,\omega_1)$ at the beginning. Unfortunately, such an approximation cannot be reasonably performed, because the self-energy $\Sigma^r(k_1,\omega_1)$ is strongly dependent on ω_1, but weakly on k_1.

Substitution of the free pole values in the Eq. (40) leads to the following Boltzmann-like equation:

$$
\begin{aligned}
iC_0\Bigg[\pm C_0 k_2 - \hbar\omega_2 + \Sigma^r\left(\frac{e_{k_1}-\mu}{\hbar}+\omega_2\right) - \Sigma^a\left(\frac{e_{k_1}-\mu}{\hbar}\right)\Bigg]\frac{\delta G^<}{\delta \mathbf{A}_\pm}\left(\frac{e_{k_1}-\mu}{\hbar};k_2,\omega_2\right)
\\
= \pm\frac{i\hbar k_F}{m}[n_F(e_{k_1}-\mu+\hbar\omega_2)-n_F(e_{k_1}-\mu)] + \int \frac{C_0\, dq_l}{2\pi\hbar}\left(\frac{n_F(e_{k_1}-\mu+\hbar\omega_2)+n_F(e_{k_1}-\mu)}{2}+n_B(e_{k_1}-e_{k_1-q_l})\right)
\\
\times\left[F_f\left(\frac{e_{k_1}-e_{k_1-q_l}}{\hbar}\right)\frac{\delta G^<}{\delta \mathbf{A}_\pm}\left(\frac{e_{k_1-q_l}-\mu}{\hbar};k_2,\omega_2\right)+F_b\left(\frac{e_{k_1}-e_{k_1-q_l}}{\hbar}\right)\frac{\delta G^<}{\delta \mathbf{A}_\mp}\left(\frac{e_{k_1-q_l}-\mu}{\hbar};k_2,\omega_2\right)\right]
\\
+ i[n_F(e_{k_1}-\mu)-n_F(e_{k_1}-\mu+\hbar\omega_2)]\int\frac{d\bar{\omega}}{2\pi}\frac{1}{e_{k_1}-\mu-\hbar\bar{\omega}}
\\
\times\int\frac{C_0\, dq_l}{2\pi}\left[F_f\left(\frac{e_{k_1}-e_{k_1-q_l}}{\hbar}\right)\frac{\delta G^<}{\delta \mathbf{A}_\pm}\left(\bar{\omega}-\frac{e_{k_1}-e_{k_1-q_l}}{\hbar};k_2,\omega_2\right)+F_b\left(\frac{e_{k_1}-e_{k_1-q_l}}{\hbar}\right)\frac{\delta G^<}{\delta \mathbf{A}_\mp}\left(\bar{\omega}-\frac{e_{k_1}-e_{k_1-q_l}}{\hbar};k_2,\omega_2\right)\right].
\end{aligned}
\tag{41}
$$

The final formula for the conductivity (37) can be changed similarly. We should also perform in (41) the linearization of the electron dispersion law, to get an agreement with the approximation applied at (33). The performed approximations are summarized in Table II (the first/second row corresponds to the forward/backward scattering). In the Appendix C a direct comparison shows that the Holstein equation in the present system is identical to (41).

D. Numerical results for two-particle properties

We have applied the transport equations (40) and (41) and the Holstein equation (C3) to the present problem. The numerical results of these equations are practically the same, so we do not distinguish between them here. The results are first discussed in physical terms. To this goal relaxation times can be used (see their definition in the Appendix D). We discuss the average time between scattering events $\langle\tau_s\rangle$ and the average momentum relaxation time $\langle\tau_p\rangle$ separately for the forward and backward scattering processes. Additional indices *forward*, *backward* are used at these times, which characterize fictitious systems with only one type of a scattering. In most situations one of the processes dominates, so that discussion of separate processes is reasonable. After the introductory summary some numerical examples are presented.

TABLE II. Scattering channels (approximate regions of parameters).

k	q_l	$e_k-e_{k-q_l}$	e_{k-q_l}
$\pm k_F$	0	$\pm C_0 q_l$	$\mu + C_0(\pm k - k_F \mp q_l)$
$\pm k_F$	$\pm 2k_F$	$\mp C_0 q_l$	$\mu + C_0(\pm k - k_F \pm q_l)$

In Fig. 1 we have seen that magnitudes of the functions $\mathrm{Im}\,\Sigma^r_{\mathrm{forward/backward}}(e_k)$ in the plateaus are of the same order. This means that the rates for relaxing electrons from their incoming states by forward and backward scattering are similar. Averaging of $1/\mathrm{Im}\,\Sigma^r_{\mathrm{forward/backward}}(e_k)$ with the distribution function $df_0(k)/de_k$, as in (D4), gives the average times between scattering events $\langle\tau_s\rangle_{\mathrm{forward/backward}}$. At high temperatures the structure in $\mathrm{Im}\,\Sigma^r_{\mathrm{forward/backward}}(e_k)$ disappears and it approximately holds $\langle\tau_s\rangle_{\mathrm{forward}} \approx \langle\tau_s\rangle_{\mathrm{backward}}$. Below $T \approx 1$ K this approximate equivalence fails, because the time $\langle\tau_s\rangle_{\mathrm{backward}}$ diverges[24] like $\exp(cT^{-1})$, due to the fact that the distribution function $df_0(k)/de_k$ does not overlap the plateaus in $\mathrm{Im}\,\Sigma^r_{\mathrm{backward}}$.

On the other hand, the electron *momentum* is relaxed by the forward and backward scattering very differently. Forward scattering does not change the sign of the electron momentum and practically preserves its magnitude ($k' \approx k$), so the momentum is relaxed very slowly. Backward scattering gives an opposite sign to the momentum and changes its magnitude slightly, so the momentum is relaxed quite fast. The different character of these scattering processes becomes evident in the conductivity or equivalently in the magnitude of the momentum relaxation time $\langle\tau_p\rangle$. Already at high temperatures the two scattering channels have very different momentum relaxation times $\langle\tau_p\rangle_{\mathrm{forward}} \gg \langle\tau_p\rangle_{\mathrm{backward}}$. At low temperatures it holds that $\langle\tau_p\rangle_{\mathrm{backward}} \approx \exp(cT^{-1})$, similarly as before.

These facts can be arranged as follows [see also comment at Fig. 1 and Eq. (D6)]. At temperatures higher than $T \approx 1$ K backward scattering dominates, so the total time $\langle\tau_p\rangle$ is suppressed approximately to the total time $\langle\tau_s\rangle$. Below $T \approx 1$ K backward scattering freezes out and forward scattering dominates. Therefore $\langle\tau_p\rangle$, given here practically only by forward

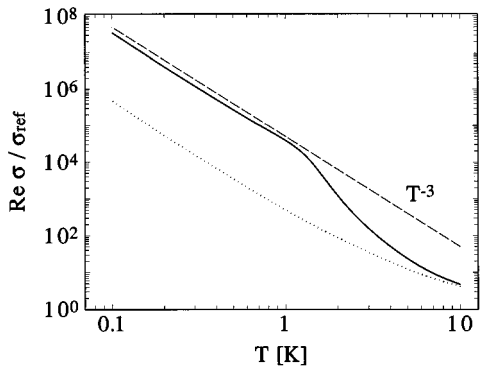


FIG. 2. The dc conductivity in the temperature interval $T=0.1-10$ K for parameters in Table I. We relate the conductivity to a reference value $\sigma_{\rm ref}=(2e^2/h)l_{\rm ref}$, where the reference length is $l_{\rm ref}=1$ μm. At higher temperatures vertex (full line) and nonvertex (dotted line) solutions coincide. In the intermediate temperatures the backward scattering freezes out and the vertex conductivity rapidly grows. Below $T\approx 1$ K only the forward scattering contributes and both solutions follow a third power law T^{-3}.

scattering, grows and becomes much larger than $\langle \tau_s \rangle$. The times $\langle \tau_s \rangle$ and $\langle \tau_p \rangle$ are approximately in the same relationship like the nonvertex and vertex conductivity. If vertex corrections to the conductivity are included in our model, they are not very important at high temperatures, while they completely renormalize the conductivity at low temperatures.

1. Homogeneous conductivity

Let us first discuss the homogeneous conductivity $\sigma(k=0,\omega)$. At high temperatures the frequency width of the distribution function $dn_F(\hbar\omega)/d\omega$ is broader than the gap in $\mathrm{Im}\,\Sigma^r_{\rm backward}(\omega)$. Therefore the backward scattering contributes to the conductivity, where it dominates over the renormalized forward scattering. The nonvertex Kubo formula gives here approximately the same dc conductivity like the transport equations. At lower temperatures the distribution function $dn_F(\hbar\omega)/d\omega$ overlaps only little with the structures in $\mathrm{Im}\,\Sigma^r_{\rm backward}(\omega)$ and the nonvertex Kubo formula fails. Below $T\approx 1$ K the distribution function is fully localized inside the gap in $\mathrm{Im}\,\Sigma^r_{\rm backward}(\omega)$, so that the backward scattering completely freezes out and the forward scattering dominates in the conductivity.[16]

In Fig. 2 we present the homogeneous dc conductivity $\sigma(k=0,\omega=0)$ in the temperature interval $T=0.1-10$ K, calculated from the transport equations (41) for the parameters from Table I. This figure clearly supports conclusions from the previous paragraphs. At higher temperatures vertex solution (full line) and nonvertex solution (dotted line) coincide. At lower temperatures backward scattering freezes out and below $T\approx 1$ K, where the forward scattering dominates, the vertex solution is about two orders bigger than the nonvertex solution. Here both solutions for the dc conductivity give a low-temperature asymptotic behavior of the form T^{-3}. The presence of the forward scattering at low temperatures changes an exponential in T behavior of the conductivity $\exp(cT^{-1})$, from freezing out backward scattering,[23,24] to a power law in T. The third power is probably a consequence of a confined geometry, which breaks down the conservation law of a momentum. Similar results can be found for the homogeneous ac conductivity $\sigma(k=0,\omega\neq 0)$.

We can also briefly comment on the numerical solution of the transport equations, solved here by iterations. The iterations have started from the nonvertex solution and the vertex corrections have been switched on very slowly, because the convergence radius is closely approached during iterations. We have multiplied the vertex part in (40) by a number, which was varied in an interval $c_{\rm iter}=0.8-0.99$ during the iterations. It is also suitable to start the next solution from the previous one and not from the new nonvertex solution.

2. Inhomogeneous conductivity

The inhomogeneous conductivity $\sigma(k\neq 0,\omega)$ is more complex. The real part of the conductivity $\mathrm{Re}\,\sigma(k,\omega)$ is a symmetric function of the excitation wave vector k, which, for a nonzero excitation frequency ω, is formed by two peaks located at $\pm k_{\rm res}$. Their position is determined by the Fermi velocity v_F as $\omega\approx v_F|k_{\rm res}|$ and their width Δk can be approximately related with the dc transport time by $\langle \tau_p \rangle \approx 2\pi/\Delta k v_F$ (the width of the nonvertex solution $\Delta_{\rm non}k$ fulfills the same relation for the time $\langle \tau_s \rangle \approx 2\pi/\Delta_{\rm non}k v_F$). As the frequency goes down $\omega\to 0$, the two peaks join each other and the total weight below the curve $\mathrm{Re}\,\sigma(k,\omega)$ can change in dependence on the type of a dominant scattering process. If only the forward scattering is present in the system, then the weight is preserved. If also the backward scattering is present, then the weight goes down (till 0 for elastically approximated backward scattering[16]). Therefore at high temperatures (backward scattering dominates) the weight falls down greatly as $\omega\to 0$ and deeply below the freezing temperature (forward scattering dominates) the weight is preserved.

In Fig. 3 we present the behavior of the k–dependent conductivity as $\omega\to 0$, calculated from the transport equations (40). The weight below the curve $\mathrm{Re}\,\sigma(k,\omega)$ is preserved for the low temperature $T=1$ K, while it goes down for $T=2$ K, where the backward scattering is present.

3. Conductance

These results are reflected in the ac conductance $\Gamma(\omega)$ [do not confuse $\Gamma(\omega)$ with usual symbols for an electron–photon or electron–phonon vertex]. The conductance could be defined[18] by an absorbed power $P(\omega)$ of a locally excited quantum wire in the electric field $E(x,\omega)$

$$\Gamma(\omega)\equiv\frac{P(\omega)}{\phi^2(\omega)/2},\quad \phi(\omega)=\int_{\rm irad.\ reg.} dx\ E(x,\omega), \quad (42)$$

where $\phi(\omega)$ is the change of the electric potential in the iradiated region. In a k representation the absorbed power can be expressed by the conductivity and the acting field as

$$P(\omega)=\frac{1}{2}\int\frac{dk}{2\pi}\,\mathrm{Re}\sigma(k,\omega)|E(k,\omega)|^2. \quad (43)$$

If the radiation falls only in a space interval of the wire with a finite length

$$E(x)=E_0[\Theta(x-L/2)-\Theta(x+L/2)],$$

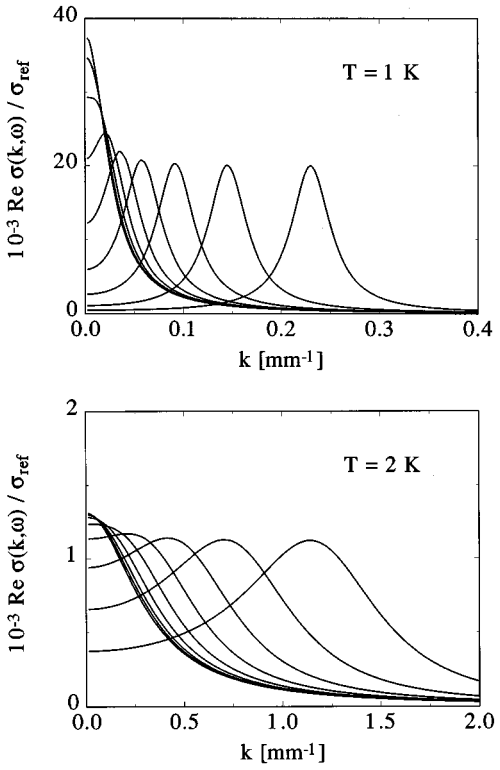


FIG. 3. The k-dependent ac conductivity for different excitation frequencies ω and the temperature $T=1,2$ K, calculated from the solution of transport equations. As this frequency grows a resonant peak forms in Re $\sigma(k,\omega)$ and moves to higher resonant wave vectors k of the excitation field. As the frequency falls down $\omega\to 0$, the surface below the curve Re $\sigma(k,\omega)$ can be reduced. In the upper drawing ($T=1$ K) backward scattering is frozen up and the surface is preserved, while on the lower drawing ($T=2$ K) the backward scattering is present and the surface is not conserved.

then the ac conductance can be expressed as

$$\Gamma(\omega)=\int \frac{dk}{2\pi}\,\mathrm{Re}\sigma(k,\omega)\left(\frac{\sin(kL/2)}{kL/2}\right)^2. \qquad (44)$$

The source with the length L has a k spectrum localized around the origin $k=0$. Therefore the conductance $\Gamma(\omega)$ in (44) becomes sensitive to the area below the curve Re $\sigma(k,\omega)$. For usual lengths L (in range of microns), the momentum width of the function $(\sin(kL/2)/(kL/2))^2$ is larger than that of Re $\sigma(k,\omega)$. Therefore the change of the surface below the curve Re $\sigma(k,\omega)$ as $\omega\to 0$ (see Fig. 3) is reflected in the conductance (44).

In Fig. 4 the dc conductance $\Gamma(\omega)$ from (44) is evaluated for the solution of the transport equations (41) or equivalently the Holstein equation (C3). The excitation source of the length $L=2\mu$m is considered. We can see that the value $2e^2/h$, characteristic for a Fermi liquid,[25] is practically reached by both vertex and nonvertex solutions as $T\to 0$. Nevertheless, recent theories and experiments support the Luttinger liquid behavior, which cannot be described by the Migdal self-energy. The onset of a backward scattering above $T\approx 1$ K is accompanied by a sharp falling down of the vertex solution. This can be understood as a blocking of the wire by consequent scattering of electrons in backward directions. The magnitude of the changed conductance is rather given by the degree of inelasticity of the backward scattering, than by the strength of this scattering. At $T\approx 5$ K the nonvertex solution suddenly falls down, because $2\pi/\Delta_{\mathrm{non}}k$ approaches the excitation length $L=2$ μm. In the vertex solutions this falling is characterized by the length $2\pi/\Delta k$. Physically, this falling down corresponds to a transfer from the ballistic in the Ohmic regime of the conductance.

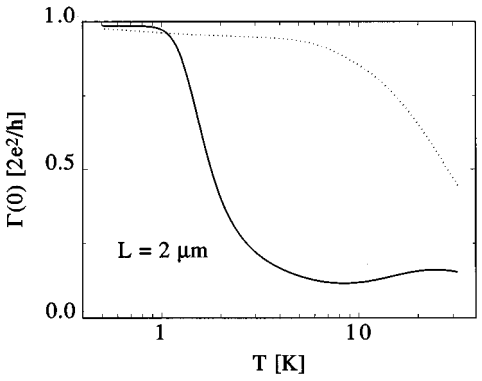


FIG. 4. The dc conductance for the vertex (full line) and nonvertex solutions (dotted line) as a function of a temperature. As $T\to 0$ both solutions approach the value $2e^2/h$. Above $T=1$ K the vertex solution sharply goes to a smaller value, determined by the inelasticity of the backward scattering, while the nonvertex solution relaxes very slowly. For a finite length $L=2$ μm a cut off is seen at some temperature in both solutions. It results from a competition of L with $2\pi/\Delta k(\Delta_{\mathrm{non}}k)$, and corresponds to a transfer in the Ohmic regime.

We have also evaluated the ac conductance, in order to see the influence of high-frequency electric fields on the blocking. The results are presented in Fig. 5. Below $T\approx 1$ K the backward scattering is frozen up and the conductance is a flat function of ω, starting from the asymptote $\Gamma(\omega=0)\approx 2e^2/h$ in Fig. 4. Above $T\approx 1$ K this asymptote falls down, since the backward scattering survives. This falling of $\Gamma(\omega)$ is disturbed by the excitation field, if its fre-

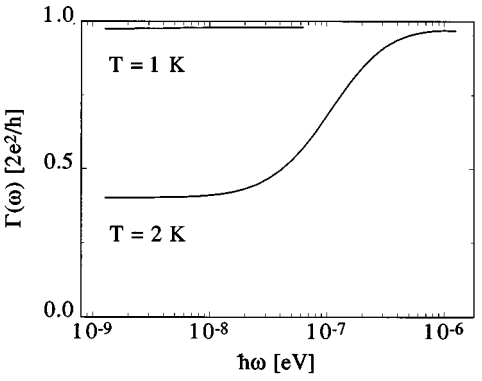


FIG. 5. The frequency-dependent ac conductance $\Gamma(\omega)$ for $T=1,2$ K. In the limit $\omega\to 0$ these curves approach the dc conductance $\Gamma(\omega=0)$ from the previous figure. At low frequencies both curves for the ac conductance $\Gamma(\omega)$ are flat. As the frequency grows, blocking at $T=2$ K becomes disturbed, so that both curves saturate to the common plateau close to $2e^2/h$. The nonvertex solution would be concave at all temperatures as $\omega\to 0$.

quency follows $\omega > v_F \Delta k/2\pi$. Therefore at $T=2$ K the ac conductance $\Gamma(\omega)$ is a convex function of frequency as $\omega \to 0$. The convexity of $\Gamma(\omega)$ has also been predicted in capacitance effects, characteristic for resonant tunneling devices.[26] The nonvertex solution,[17] which is a flat concave function of frequency as $\omega \to 0$, is not presented here. At higher frequencies interference dips[17] from the finite length of excitation $L=2$ μm might appear in all solutions.

In experiments usually a short channel is connected to broad contacts. Then a conductance defined from a transmissivity of this short channel[27] probably does not fall down as much as in Fig. 4. This is because, in experiments, backward scattering of electrons in the ballistic regime usually takes part outside of the short channel. The scattered electrons do not return back to this short channel, but spread out in the contacts. As a result the Fermi level in the constriction is not well stabilized against shift by the electric field, and blocking is not possible. In more realistic calculations screening should be also included. Our nonscreened results correspond only to the drifted part of the total conductivity.[28]

IV. CONCLUSION

We have developed[29] a linear response method for quantum many-body systems by linearization of the nonequilibrium Green's function equations[1] in the integral form. The linearized integral equations result in a simpler way than the linearized differential equations,[11] because some transforms can be avoided. In the new method also the one- and two-particle points of view are very closely interconnected. Therefore the method is more direct than the Kubo formula, where vertex equations of different analytical structures must be solved in the first step.

As a demonstration example, we have calculated a linear response of a quantum wire with an electron–phonon interaction to longitudinal electric fields.[29] After application of standard approximations from metals to the linearized equations, we have obtained the Holstein equation,[12] being a weak scattering limit of the Kubo formula in the present problem. The Holstein equation has been solved, and from its solutions the ac/dc conductivity have been calculated. We have realized that for high temperatures $T \gg 1$ K the solution of the nonvertex Kubo formula[17] agrees with the Holstein equation. At lower temperatures the scattering of electrons in a backward direction freezes out and for temperatures $T<1$ K the forward scattering completely dominates. Here both the solution of the nonvertex Kubo formula and the Holstein equation go like T^{-3}, but the vertex solution of the Holstein equation gives a much larger conductivity. Similar effects have been found in the ac conductivity for homogeneous or inhomogeneous probe electric fields.

These results have been applied to evaluation of the ac/dc conductance, calculated from a locally absorbed power by the system.[18] The one channel dc conductance approaches its ballistic value $2e^2/h$ below $T \approx 1$ K. Above this temperature the dc conductance sharply decreases, since the backward scattering becomes active. This blocking of the transport by the backward scattering is disturbed, if frequencies of the excitation field are bigger than the backward scattering rate.

We believe that the new method, introduced and tested here, can be applied in more complicated linear response problems. The method could be systematically generalized to probe stationary nonequilibrium[31] or nonstationary systems.[6] A nonlinear response of quantum systems could be defined by higher-order functional derivatives over external fields.

ACKNOWLEDGMENTS

The author would like to thank B. Velický for wide support of this project and for many stimulating discussions. He is also grateful to P. Lipavský, V. Špička, and J. Mašek for discussions of the formalism and many helpful comments. The numerical part of this work has been done on CRAY Y-MP EL at the Institute of Physics and on STARDENT in ASCOC Laboratory, Prague.

APPENDIX A: SUMMARY OF GREEN'S FUNCTIONS

In this appendix we define Green's functions for real times (analogously, the Matsubara Green's functions can be defined in complex times). Some standard relationships between functions with different analytical structures are also introduced.

The causal (time-ordered) fermion ($O=\psi$) or boson ($O=A$) Green's functions[20] are defined by

$$G^t(1,2) = -\frac{i}{\hbar}\langle T[O(1)O^\dagger(2)]\rangle, \quad j \equiv (\mathbf{r}_j, t_j) \quad (j=1,2). \tag{A1}$$

Correlation functions are related to the causal functions by

$$\begin{aligned} i\hbar G^t(1,2) &= G^>(1,2) = \langle O(1)O^\dagger(2)\rangle, \quad t_1 > t_2, \\ \mp i\hbar G^t(1,2) &= G^<(1,2) = \langle O^\dagger(2)O(1)\rangle, \quad t_1 < t_2, \end{aligned} \tag{A2}$$

where the upper (lower) sign applies for fermions (bosons). The retarded and advanced Green's functions are defined by

$$\begin{aligned} G^r(1,2) &= -\frac{i}{\hbar}\theta(1-2)[G^>(1,2) \pm G^<(1,2)], \\ G^a(1,2) &= \frac{i}{\hbar}\theta(2-1)[G^>(1,2) \pm G^<(1,2)]. \end{aligned} \tag{A3}$$

In space homogeneous systems the Green's functions depend only on the difference $\mathbf{r}=\mathbf{r}_1-\mathbf{r}_2$, so that in the k representation they result as

$$\begin{aligned} G^t(\mathbf{k};t_1,t_2) &\equiv \int_{-\infty}^{\infty} d^n\mathbf{r} e^{-i\mathbf{r}\cdot\mathbf{k}} G^t(\mathbf{k};t_1,t_2) \\ &= -\frac{i}{\hbar(2\pi)^n}\langle T[O(\mathbf{k},t_1)O^\dagger(\mathbf{k},t_2)]\rangle. \end{aligned} \tag{A4}$$

Here the operator is equal to $O(\mathbf{k},t)=a_{\mathbf{k}}(t)$ or $O(\mathbf{k},t)=b_{\mathbf{q}}(t)+b^+_{-\mathbf{q}}$ for fermions or bosons. In a thermodynamic equilibrium they depend also on the difference $t=t_1-t_2$, and after a Fourier transform over times the fermion and boson correlation functions read[1]

$$G^{<}(k,\omega)=n_{F,B}(\hbar\omega)A_G(k,\omega),$$
$$G^{>}(k,\omega)=(1\mp n_{F,B}(\hbar\omega))A_G(k,\omega), \tag{A5}$$

where n_F, n_B denote the Fermi-Dirac and Bose-Einstein distributions

$$n_{F,B}(\hbar\omega)=\frac{1}{e^{\hbar\omega/kT}\pm 1}$$

and the spectral function is defined by

$$A_G(k,\omega)\equiv -2\ \mathrm{Im}\ G^r(k,\omega)=G^{>}(k,\omega)\pm G^{<}(k,\omega). \tag{A6}$$

From Kramers-Kronig rules it follows that the retarded fermion or boson Green's function can be calculated from its spectral function (A6) by

$$G^r(k,\omega)=\int_{-\infty}^{\infty}\frac{d\bar{\omega}}{2\pi}\frac{A_G(k,\bar{\omega})}{\omega-\bar{\omega}+i\delta}. \tag{A7}$$

Most of the above formulas hold not only for the Green's function but also for the self-energy. For example the spectral function for the self-energy can be represented by correlation functions for the self-energy as in (A5). Then the retarded self-energy can be found from its spectral function by (A7).

The nonequilibrium Green's functions are derived by analytical continuation of the Matsubara Green's functions in complex times.[1] In NGF it is often necessary to find the retarded or small part of a combination of functions in complex times. An example is the product

$$A(1,2)=-iB(1,2)C(1,2), \tag{A8}$$

where A,B,C are one-particle causal Green's functions or self-energies and the numbers with bars mean that these pairs of coordinates are integrated out. The required functions can be found by analytical continuation along a complex curve[5] and reduction to the real axis

$$A^{<}(1,2)=B^{<}(1,2)C^{<}(1,2),$$
$$A^{r}(1,2)=B^{r}(1,2)C^{<}(1,2)+B^{<}(1,2)C^{a}(1,2). \tag{A9}$$

Other structures can be handled similarly. The integral version of the Dyson equation leads to the following equation for the nonequilibrium correlation function (equation for $G^{>}$ results by the exchange of signs $<$ and $>$ here):

$$G^{<}(1,2)=G^{r}(1,\bar{3})(G_0^{-1})^{r}(\bar{3},\bar{4})G_0^{<}(\bar{4},\bar{5})\times(G_0^{-1})^{a}(\bar{5},\bar{6})G^{a}(\bar{6},2)+G^{r}(1,\bar{3})\Sigma^{<}(\bar{3},\bar{4})G^{a}(\bar{4},2). \tag{A10}$$

The nonequilibrium propagators $G^{r,a}$ can be found from $G^{<,>}$ by (A3).

APPENDIX B: FULFILLMENT OF CONSERVATION LAWS

Here we present an analog of *generalized Ward identities*[9] for the linearized functions $\delta G^{<}/\delta U$, which can be applied to prove conservation laws[31] for these functions. The derivation is the same as for the linear response function $L(1,2;3,4)$, used in standard approaches.[9,31]

Consider that electric and magnetic fields acting on the studied quantum system are zero. The scalar and vector potentials, coupled by a gauge transform, can still be nonzero. This equilibrium system can be described by differential equations for $G^{<,>}$ in the presence of the potentials[11]

$$\mathbf{A}(r,t)=\nabla\Lambda(r,t),\quad \phi(r,t)=-\frac{1}{c}\frac{\partial}{\partial t}\Lambda(r,t), \tag{B1}$$

for any reasonable gauge function $\Lambda(r,t)$.

The solution of these equations can be expressed as[9]

$$G^{<,>}(1,2;\Lambda)=\exp[-\Lambda(1)]G^{<,>}(1,2;\Lambda=0)\exp[\Lambda(2)], \tag{B2}$$

which can be checked by the substitution of (B2) into the equations for $G^{<,>}$. The same solution should result from the integral form of these equations (A10).

Variation of $G^{<}$ in (B2) over the gauge function Λ gives (analogical expression results for $G^{>}$)

$$\left.\frac{\delta G^{<}(1,2;\Lambda)}{\delta\Lambda(3)}\right|_{\Lambda=0}=(\delta(2-3)-\delta(1-3))G^{<}(1,2;\Lambda=0). \tag{B3}$$

From the other side, for an infinitesimal change of the gauge, the change of $G^{<}$ in the potentials (B1) is equal to

$$\delta G^{<}(1,2;\Lambda)=\int d3\left[\frac{\delta G^{<}(1,2)}{\delta\phi(3)}\left(-\frac{1}{c}\frac{\partial}{\partial t_3}\Lambda(3)\right)+\frac{\delta G^{<}(1,2)}{\delta\mathbf{A}(3)}\cdot\nabla_3\Lambda(3)\right]. \tag{B4}$$

After the per-parts integration in (B4), the variation results as

$$\left.\frac{\delta G^{<}(1,2;\Lambda)}{\delta\Lambda(3)}\right|_{\Lambda=0}=\frac{1}{c}\frac{\partial}{\partial t_3}\frac{\delta G^{<}(1,2)}{\delta\phi(3)}-\nabla_3\cdot\frac{\delta G^{<}(1,2)}{\delta\mathbf{A}(3)}. \tag{B5}$$

The two variations (B3), (B5) must be equal. Therefore we get the following analog of *generalized Ward identities*:[9]

$$\frac{1}{c}\frac{\partial}{\partial t_3}\frac{\delta G^{<}(1,2)}{\delta\phi(3)}-\nabla_3\cdot\frac{\delta G^{<}(1,2)}{\delta\mathbf{A}(3)}=(\delta(2-3)-\delta(1-3))G^{<}(1,2),\quad \Lambda=0, \tag{B6}$$

which can also be interpreted as a number (charge) conservation law,[31] obeyed by the linearized functions $\delta G^{<}/\delta U$. Similarly, other laws can be derived.

APPENDIX C: COMPARISON WITH THE HOLSTEIN EQUATION

In this appendix Eq. (41) is compared with the Holstein equation,[12] which results by application of the Kubo formula to the electron–phonon interaction in metals. Holstein applies the Migdal approximation of the electron self-energy,

but does not exclude its momentum dependence. His equations result from pole approximations in a vertex equation, which can be then inverted to a transport-like form. This equation can be identified with a linearized Boltzmann equation in the limit of small external frequencies.

In the Holstein work[12] the momentum k is bound to the pole energy e_k as $\Sigma(k,(e_k-\mu)/\hbar)$. Then the transport equation can be written as follows:

$$i\left[\hbar v_k q-\hbar\omega+\Sigma^r\left(k,\frac{e_k-\mu}{\hbar}+\omega\right)-\Sigma^a\left(k,\frac{e_k-\mu}{\hbar}\right)\right]\phi_k = v_k - i\sum_{q_l} F_s(k,k-q_l)\phi_{k-q_l}, \tag{C1}$$

where the function F_s in (61) results from the vertex equation. For our problem F_s reads

$$\begin{aligned} F_s(k,k-q_l) = \sum_{q_t} |V_q|^2 \Bigg(& \frac{n_F(e_{k-q_l}-\mu)+n_B(\hbar\omega_q)}{e_k-e_{k-q_l}+\hbar\omega_q-i\delta} + \frac{1-n_F(e_{k-q_l}-\mu)+n_B(\hbar\omega_q)}{e_k-e_{k-q_l}-\hbar\omega_q-i\delta} \\ & - \frac{n_F(e_{k-q_l}-\mu+\hbar\omega)+n_B(\hbar\omega_q)}{e_k-e_{k-q_l}+\hbar\omega_q+i\delta} - \frac{1-n_F(e_{k-q_l}-\mu+\hbar\omega)+n_B(\hbar\omega_q)}{e_k-e_{k-q_l}-\hbar\omega_q+i\delta}\Bigg) \\ = & [n_F(e_{k-q_l}-\mu+\hbar\omega)-n_F(e_{k-q_l}-\mu)]P\int_{-\infty}^{\infty}\frac{d\hbar\bar\omega}{2\pi}\frac{\mathscr{A}(q_l,\bar\omega)}{e_k-e_{k-q_l}-\hbar\bar\omega} \\ & + \frac{i}{2}\mathscr{A}\left(q_l,\frac{e_k-e_{k-q_l}}{\hbar}\right)[2+2n_B(e_k-e_{k-q_l})-n_F(e_{k-q_l}-\mu)-n_F(e_{k-q_l}-\mu+\hbar\omega)]. \end{aligned} \tag{C2}$$

In the second expression some algebra has been used, which together with summation of the transversal momentum q_t in the product $\Sigma_{q_t}|V(q)|^2\delta(\cdots)$ gives the effective spectral distribution (28). Therefore the integration over $\bar\omega$ in (C2) should be performed at the end. As a result the above formulas and the following equation (C3) look rather differently than in Ref. 12.

To explicitly compare the equations (C1) and (41), we must perform in (C1) approximations analogical those done in (41). When the pole substitution $\hbar\bar\omega_1\approx e_{k_1}-e_{k_1-q_l}$ is performed in the exponent of the function $\mathscr{A}$ from (28), then in this exponent the momentum q_l appears in two places $((e_{k_1}-e_{k_1-q_l})/\hbar s)^2-q_l^2$. This function is approximated by giving the momentum q_l at the end of this expression (q_l^2) the value $q_l=0$ ($q_l=2k_F$) for the forward (backward) scattering. The same substitutions can be performed in the exponents of the expression (C2).

After these approximations of $\mathscr{A}$, the expression (C2) can be substituted in the Holstein equation (C1). We can also neglect the small difference between our $\Sigma^r((e_k-\mu)/\hbar)$ and $\Sigma^r(k,(e_k-\mu)/\hbar)$ in (C1). Then the approximated equation results

$$\begin{aligned} & i\left[\pm C_0k_2-\hbar\omega_2+\Sigma^r\left(\frac{e_{k_1}-\mu}{\hbar}+\omega_2\right)-\Sigma^a\left(\frac{e_{k_1}-\mu}{\hbar}\right)\right]\phi_\pm\left(\frac{e_{k_1}-\mu}{\hbar};k_2,\omega_2\right) \\ & = \pm v_k + \int\frac{dq_l}{2\pi\hbar}\left(-\frac{n_F(e_{k_1-q_l}-\mu)+n_F(e_{k_1-q_l}-\mu+\hbar\omega_2)}{2}-n_B(e_{k_1-q_l}-e_{k_1})\right) \\ & \times\left[F_f\left(\frac{e_{k_1}-e_{k_1-q_l}}{\hbar}\right)\phi_\pm\left(\frac{e_{k_1-q_l}-\mu}{\hbar};k_2,\omega_2\right)+F_b\left(\frac{e_{k_1}-e_{k_1-q_l}}{\hbar}\right)\phi_\mp\left(\frac{e_{k_1-q_l}-\mu}{\hbar};k_2,\omega_2\right)\right] \\ & - i\int\frac{dq_l}{2\pi}[n_F(e_{k_1-q_l}-\mu+\hbar\omega_2)-n_F(e_{k_1-q_l}-\mu)]\int\frac{d\bar\omega}{2\pi}\frac{1}{e_{k_1}-e_{k_1-q_l}-\hbar\bar\omega} \\ & \times\left[F_f(\bar\omega)\phi_\pm\left(\frac{e_{k_1-q_l}-\mu}{\hbar};k_2,\omega_2\right)+F_b(\bar\omega)\phi_\mp\left(\frac{e_{k_1-q_l}-\mu}{\hbar};k_2,\omega_2\right)\right]. \end{aligned} \tag{C3}$$

The relation between the distribution function in Ref. 12 and here is $\phi_{\pm k}\equiv\phi_{\pm}((e_k-\mu)/\hbar)$, where ϕ_k resp. ϕ_{-k} correspond to $k>0$ resp. $k<0$.

The conductivity can be found as in Ref. 12

$$\sigma(q,\omega)=2e^2\int_{\pm k}\frac{dk}{2\pi}v_{\pm k}\phi_{\pm}\left(\frac{e_k-\mu}{\hbar};q,\omega\right)\times\frac{n_F(e_{\pm k}-\mu)-n_F(e_{\pm k}-\mu+\hbar\omega)}{\omega}. \quad \text{(C4)}$$

The linearization of the electron dispersion law from Table II must be also performed in (C3) and (C4).

In order to show that Eq. (C3) is identical to the linearized transport equation (41), it is necessary to compare all terms from these equations. The following identification can be found either from (41), (C3) or from the conductivity formulas (37), (C4):

$$C_0\frac{\delta G^{<}}{\delta\mathbf{A}_{\pm}}\left(\frac{e_{k_1}-\mu}{\hbar};k_2,\omega_2\right)=i\phi_{\pm}\left(\frac{e_{k_1}-\mu}{\hbar};k_2,\omega_2\right)\times[n_F(e_{k_1}-\mu+\hbar\omega_2)-n_F(e_{k_1}-\mu)]. \quad \text{(C5)}$$

If this substitution (C5) is performed in (41), and Eq. (C3) is multiplied by $i[n_F(e_{k_1}-\mu+\hbar\omega_2)-n_F(e_{k_1}-\mu)]$, then both these equations can be directly compared. Since the left sides are evidently the same, we have to compare the right sides.

Let us compare first the leading (first) terms of the right-hand sides in these equations. If the seemingly different statistical factors are equivalent, then these terms are identical. These statistical factors in the first terms of the right-hand sides of (41) and (C3) look as follows:

$$\left(\frac{n_F(e_{k_1}-\mu+\hbar\omega_2)+n_F(e_{k_1}-\mu)}{2}+n_B(e_{k_1}-e_{k_1-q_l})\right)\times(n_F(e_{k_1-q_l}-\mu+\hbar\omega_2)-n_F(e_{k_1-q_l}-\mu)),$$

$$-\left(\frac{n_F(e_{k_1-q_l}-\mu+\hbar\omega_2)+n_F(e_{k_1-q_l}-\mu)}{2}+n_B(e_{k_1-q_l}-e_{k_1})\right)(n_F(e_{k_1}-\mu+\hbar\omega_2)-n_F(e_{k_1}-\mu)). \quad \text{(C6)}$$

The equivalency of these factors can be proven in several steps. The expressions in (C6) can be multiplied by all different denominators with exponentials from the distributions n_F, n_B. Then all terms with different powers of $\exp(\beta(e_{k_1}-e_{k_1-q_l})/\hbar)$ can be compared. After some algebra the equivalency of factors in (C6) results.

The last (renormalization) terms in Eqs. (41) and (C3) have to be compared in a different way, because the distribution functions have different arguments. After a detailed analysis, where the same integration variables are chosen, the two terms result as equivalent, too.

APPENDIX D: EVALUATION OF RELAXATION TIMES

In practice the *relaxation time approximation* of the Boltzmann equation is broadly employed.[20,32,33] In this Appendix we would like to mention this approximation in the context of linear response methods.

The relaxation time approximation can be introduced in the Boltzmann equation as follows:[20]

$$\frac{\partial f(k)}{\partial t}+\mathbf{v}\cdot\nabla f(k)+\frac{\partial\mathbf{k}}{\partial t}\cdot\nabla_k f(k)=\left(\frac{\partial f(k)}{\partial t}\right)_{\text{collis.}}\approx-\frac{f(k)-f_0(k)}{\tau_p(k)}. \quad \text{(D1)}$$

In systems which are close to equilibrium the time $\tau_p(k)$ can be identified with the (equilibrium) transport time or equivalently the momentum relaxation time.[33] Then the two right sides in (D1), i.e., the exact scattering integral and the relaxation time approximation with $\tau_p(k)$, give in most situations equivalent descriptions of the Boltzmann equation. Therefore close to equilibrium the time $\tau_p(k)$ can be directly evaluated from the equation (D1), as described below.

In systems with an isotropic dispersion law for electrons the electron momenta change in a static homogeneous electric field as $\partial\hbar\mathbf{k}/\partial t=-e\mathbf{E}$. Therefore the solution of (D1) is of the form

$$f(k)\equiv f_0(k)+\frac{e}{\hbar}\tau_p(k)\mathbf{E}\cdot\nabla_k f(k)\approx f_0(k)+\frac{e}{\hbar}\tau_p(k)\mathbf{E}\cdot\nabla_k f_0(k). \quad \text{(D2)}$$

The second expression in (D2) is an *Ansatz* for the distribution function $f(k)$, which assumes that the electric field $\mathbf{E}$ is weak.[20,32] If this *Ansatz* function $f(k)$ is substituted into the exact scattering integral $(\partial f(k)/\partial t)_{\text{collis.}}$ in (D1), then the time $\tau_p(k)$ can be evaluated from (D1). Holstein has applied this approach when compared his formulas[12] with the linearized Boltzman equation. There the function ϕ_k is considered instead of $\tau_p(k)$.

The transport time $\tau_p(k)$ is different from the time between scattering events $\tau_s(k)$, which is an inverse imaginary part of a self-energy in a pole approximation, multiplied by two. An expression for $\tau_s(k)$ can also results from Eq. (D1), if *outcoming* terms are preserved there, but *incoming* terms are neglected in the scattering integral[32] ($\approx$ the nonvertex Kubo formula). For elastic scattering the two times differ by an important factor $1-\cos\theta'=1-\mathbf{k}\cdot\mathbf{k}'/k^2$, averaged over the outcoming momenta k' with the square of the matrix element.[20] This difference expresses the fact that vertex corrections for a conductivity are included in evaluation of $\tau_p(k)$ but not in $\tau_s(k)$.

The linearized *Ansatz* (D2) can also be directly used for evaluation of an induced current in the weak field[20] $\mathbf{E}$

$$\mathbf{J}=-en_0=-en_0\int\frac{d^3k}{(2\pi)^3}f(k)\frac{\hbar\mathbf{k}}{m}$$
$$=-e^2n_0\int\frac{d^3k}{(2\pi)^3}\tau_p(k)\mathbf{v}_k(\mathbf{E}\cdot\mathbf{v}_k)\frac{df_0(k)}{de_k}. \tag{D3}$$

From (D3) a homogeneous dc conductivity in the relaxation time approximation can be defined[20]

$$\sigma=-\frac{e^2n_0}{3}\int\frac{d^3k}{(2\pi)^3}v_k^2\tau_p(k)\frac{df_0(k)}{de_k}. \tag{D4}$$

In a free electron metal at zero temperature only the electrons on the Fermi surface contribute to the transport. Then the dc conductivity (D4) gets a simple form[20]

$$\sigma=\frac{e^2n_0\tau_p(k_F)}{m}. \tag{D5}$$

At nonzero temperatures $\tau_p(k)$ is averaged by the distribution function $df_0(k)/de_k$ in (D4), so that the time $\tau_p(k_F)$ in (D5) should be substituted by the *average* transport time $\langle\tau_p\rangle$. Only at very high temperatures might the averaging again become trivial. There $\tau_p(k)$ is usually weakly k dependent and it can be taken out of the integral (D4). At high temperatures also the vertices could be less important, since scattering into all angles should become possible for energetical reasons. Therefore the substitution of $\tau_p(k)$ by $\tau_s(k)$ might be reasonable.

From the similarity of the formula (D4) with (37), it follows that an effective transport time $\tau_p(k)$ can be defined directly from the Holstein equation (C3) or from our transport equations (41) [see (C5)]. In homogeneous dc electric fields this time $\tau_p(k)$ results

$$\tau_p(k)\equiv-\frac{\hbar\phi_k}{v_k}=\frac{i\hbar C_0}{v_k}\lim_{\omega\to0}\left[\frac{1}{n_F(e_k-\mu+\hbar\omega)-n_F(e_k-\mu)}\times\frac{\delta G^<}{\delta\mathbf{A}_+}\left(\frac{e_k-\mu}{\hbar};0,\omega\right)\right]. \tag{D6}$$

If the nonvertex solution is used in the expressions (D6), then the relaxation time between scattering events $\tau_s(k)$ results instead of $\tau_p(k)$.

We can briefly discuss also the homogeneous ac conductivity, which is often described by a Drude formula. This formula applies the relaxation time approximation in ac fields as follows:

$$\sigma\approx-\frac{e^2n_0}{3}\int\frac{d^3k}{(2\pi)^3}v_k^2\frac{\tau_p(k)}{1-i\omega\tau_p(k)}\frac{df_0(e_k)}{de_k}$$
$$\approx\frac{n_0e^2}{m}\frac{\langle\tau_p\rangle}{1-i\omega\langle\tau_p\rangle}. \tag{D7}$$

The first expression in (D7) can be obtained from the Boltzmann equation (D1) in the same way as (D4). The ac *Ansatz* differs from (D2) by the multiplicative factor $1/[1-i\omega\tau_p(k)]$ in the right side of (D2). In a more exact approach the second expression in (D7) should be written as $\langle\tau_p(k)/[1-i\omega\tau_p(k)]\rangle$.

Numerical results for the ac conductivity seem to fulfill the Drude formula (D7) for some time $\tau_p(k)$. Therefore we could try to define the new ac relaxation time from (D7) similarly as in (D6) (the condition is $\hbar\omega\ll kT$)

$$\frac{\tau_p(k)}{1-i\omega\tau_p(k)}\equiv-\frac{\hbar\phi_k}{v_k}$$
$$=\frac{i\hbar C_0}{v_k}\left[\frac{1}{n_F(e_k-\mu+\hbar\omega)-n_F(e_k-\mu)}\times\frac{\delta G^<}{\delta\mathbf{A}_+}\left(\frac{e_k-\mu}{\hbar};0,\omega\right)\right]. \tag{D8}$$

Here the solutions of transport equations in homogeneous ac electric fields should be substituted. The relaxation time could depend also on the external frequency $\tau_p(k,\omega)$.[20] The definition (D8) is not applicable, when $\tau_p(k,\omega)$ appears to be complex (or the imaginary part is relatively big). Then the Drude-like formula is not valid.

[1] L. P. Kadanoff and G. Baym, *Quantum Statistical Mechanics* (Benjamin, New York, 1962).

[2] L. V. Keldysh, Zh. Éksp. Teor. Fiz. **47**, 1515 (1964) [Sov. Phys. JETP **20**, 1018 (1965)].

[3] NGF was applied in many areas of quantum transport; examples are C. Caroli, R. Combescot, P. Nozieries, and D. Saint-James, J. Phys. C **5**, 21 (1972); D. C. Langreth and J. W. Wilkins, Phys. Rev. B **6**, 3189 (1972); K. Henneberger and H. Haug, *ibid.* **38**, 9759 (1988); H. Shao, D. C. Langreth, and P. Nordlander, *ibid.* **49**, 13 929 (1994); **49**, 13 948 (1994).

[4] P. Lipavský, V. Špička, and B. Velický, Phys. Rev. B **34**, 6933 (1986).

[5] D. C. Langreth, in *Linear and Nonlinear Electron Transport in Solids*, edited by J. T. Devresee and E. van Boren (Plenum, New York, 1976).

[6] A. P. Jauho, Phys. Rev. B **32**, 2248 (1985).

[7] R. Kubo, J. Phys. Soc. Jpn. **12**, 570 (1957).

[8] T. Matsubara, Prog. Theor. Phys. (Kyoto) **14**, 351 (1955).

[9] G. Strinati, Riv. Nuovo Cimento **11** (12), 1 (1988).

[10] R. E. Prange and L. P. Kadanoff, Phys. Rev. **134**, A566 (1964).

[11] W. Hänsch and G. D. Mahan, Phys. Rev. B **28**, 1902 (1983).

[12] T. Holstein, Ann. Phys. **29**, 410 (1964).

[13] L. Y. Chen and Z. B. Su, Phys. Rev. B **40**, 9309 (1989).

[14] J. W. Wu and G. D. Mahan, Phys. Rev. B **29**, 1769 (1984).

[15] M. Levanda and V. Fleurov, J. Phys. Condens. Matter **6**, 7889 (1994).

[16] The present paper forms a major part of the Ph.D. thesis of P. Král, Institute of Physics, Prague, 1995.

[17] V. Špička, J. Mašek, and B. Velický, J. Phys. Condens. Matter **2**, 1569 (1990).

[18] D. S. Fisher and P. A. Lee, Phys. Rev. B **23**, 6851 (1981); B. Velický, J. Mašek, and B. Kramer, Phys. Lett. A **140**, 447 (1989).

[19] G. Baym, Phys. Rev. **127**, 1391 (1962).
[20] G. D. Mahan, *Many Particle Physics* (Plenum, New York 1981).
[21] B. Velický, V. Špička, and J. Mašek, Solid State Commun. **72**, 981 (1989).
[22] A. B. Migdal, Zh. Éksp. Teor. Fiz. **34**, 1438 (1958).
[23] J. R. Senna and S. Das Sarma, Phys. Rev. Lett. **70**, 2593 (1993).
[24] H. Bruus, K. Flensberg, and H. Smith, Phys. Rev. B **48**, 11 144 (1993).
[25] C. L. Kane and M. P. Fischer, Phys. Rev. Lett. **68**, 1220 (1992).
[26] T. Brandes, D. Weinmann, and B. Kramer, Europhys. Lett. **22**, 51 (1993).
[27] R. Landauer, IBM J. Res. Dev. **1**, 223 (1957).
[28] J. L. Warren and R. A. Ferrell, Phys. Rev. **117**, 1252 (1960).
[29] P. Král, *Quantum Transport in Ultrasmall Devices*, edited by D. K. Ferry, H. L. Grubin, C. Jacoboni, and A. P. Jauho (Plenum, New York, 1995), p. 529.
[30] Y. Meir and N. S. Wingreen, Phys. Rev. Lett. **68**, 2512 (1992); N. S. Wingreen, A. P. Jauho, and Y. Meir, Phys. Rev. B **48**, 8487 (1993).
[31] G. Baym and L. P. Kadanoff, Phys. Rev. **124**, 287 (1961).
[32] H. Smith and H. H. Jensen, *Transport Phenomena* (Clarendon, Oxford, 1989).
[33] V. F. Gandmacher and Y. B. Levinson, in *Modern Problems in Condensed Matter Sciences*, edited by V. M. Agranovich and A. A. Maradudin (North-Holland, New York, 1987), Vol. 19.